

Optimal Control of Distributed Energy Resources using Model Predictive Control

Ebony Mayhorn, *Student Member, IEEE*, Karanjit Kalsi, *Member, IEEE*, Marcelo Elizondo, *Member, IEEE*, Wei Zhang, *Member, IEEE*, Shuai Lu, *Member, IEEE*, Nader Samaan, *Member, IEEE*, Karen Butler-Purry, *Senior Member, IEEE*

Abstract — In an isolated power system (rural microgrid), distributed energy resources (DERs), such as renewable energy resources (wind, solar), energy storage and demand response, can be used to complement fossil fueled generators. The uncertainty and variability due to high penetration of wind makes reliable system operations and controls challenging. In this paper, an optimal control strategy is proposed to coordinate energy storage and diesel generators to maximize wind penetration while maintaining system economics and normal operation performance. The problem is formulated as a multi-objective optimization problem with the goals of minimizing fuel costs and changes in power output of diesel generators, minimizing costs associated with low battery life of energy storage, and maximizing the ability to maintain real-time power balance during operations. Two control modes are considered for controlling the energy storage to compensate either net load variability or wind variability. Model predictive control (MPC) is used to solve the aforementioned problem and the performance is compared to an open-loop look-ahead dispatch problem under high penetration of wind. Simulation studies using different prediction horizons further demonstrate the efficacy of the closed-loop MPC in compensating for uncertainties in the system caused by wind and demand.

Index Terms— model predictive control, coordination of distributed energy resources

NOMENCLATURE

| | |
|----------------|--|
| $C(P_{Gi}(k))$ | fuel cost for diesel unit i at time step k (\$) |
| $P_{Gi}(k)$ | scheduled output level of diesel generator i at time step k (kW) |
| P_{Gi}^{min} | minimum rated power of generator i |
| P_{Gi}^{max} | maximum rated power of generator i |
| R_{Gi}^{max} | maximum ramp rate of generator i |
| G | set of all diesel generators |
| $C(P_s(k))$ | cost of operating the Battery Energy Storage System (BESS) |
| $SOC(k)$ | State of Charge of BESS at time step k |
| π_{SOC} | penalty factor on low State of Charge (SOC) |
| SOC_{ref} | reference state of charge |
| $P_s(k)$ | BESS charge/discharge power level at time step |

| | |
|--------------------|--|
| E_{max} | k (MW) |
| η | energy capacity of BESS (kWh) |
| SOC_{min} | efficiency of BESS |
| SOC_{max} | minimum SOC of BESS |
| $T(k)$ | maximum SOC of BESS |
| $P_L(k)$ | threshold used as control input to compensate for wind or net load variability |
| $P_w(k)$ | actual load power at time step k |
| $\hat{P}_{Gi}(k)$ | actual wind power at time step k |
| $\widehat{SOC}(k)$ | predicted power of diesel generator i at time step k |
| $\hat{T}(k)$ | predicted SOC of BESS at time step k |
| $\hat{P}_L(k)$ | predicted threshold value |
| $\hat{P}_w(k)$ | forecasted load power at time step k |
| Gr | forecasted wind power at time step k |
| | set of all wind generators |

I. INTRODUCTION

ISOLATED power systems are typically small distribution systems in remote areas, which lack support from larger interconnected power grids. In these systems, electricity is often supplied by small fossil fueled generators that tend to be very expensive to operate. Integrating distributed energy resources (DERs), such as renewable resources and energy storage, can allow for economical and environmentally friendly operation. However, there is significant variability and uncertainty associated with high penetration of renewable resources like wind and solar. Energy storage devices have inter-temporal constraints associated with their operation, and it can be difficult to predict the state of charge (SOC) during operation of some energy storage devices. Due to these inherent characteristics of wind and energy storage, real-time operations and control coordination becomes challenging.

Many centralized/decentralized control strategies have been and are being developed to integrate DERs in power system operations. Examples of control strategies already proposed and/or developed such as the ‘Grid Friendly Appliance’ technology (decentralized) is given in [1]. A decentralized droop control is added to disaggregated loads using quasi-continuous control law to have a desired aggregated response for frequency and stability control in [2]. In [3], a decentralized control of voltage profile is proposed in the distribution system with DGs using reactive power control of inverters. A centralized AGC-type control of DGs is proposed in [4]. A combination of centralized and decentralized coordination strategies for a rural microgrid, containing wind and diesel generators, BESS, and demand response, were studied in [5]. The objectives for the coordination strategies were to maintain system frequency close to nominal and to reduce fossil fuel generator movement by allowing energy

This work was supported by the Laboratory Directed Research and Development (LDRD) program at the Pacific Northwest National Laboratory.

E. Mayhorn and K. Butler-Purry are with Texas A&M University, College Station, TX.

K. Kalsi, M. Elizondo, S. Lu and N. Samaan are with Pacific Northwest National Laboratory, Richland, WA 99354 USA.

W. Zhang is with the Ohio State University, Columbus, OH

storage devices to compensate wind variability. Arbitrary control inputs were selected only to show the effectiveness of the control coordination strategies. The authors recognized the need for an optimally coordinated control scheme between different DERs.

Several coordination strategies of DERs, to provide ancillary services (i.e., scheduling, dispatch, balancing, contingency response, etc.) have been explored in [6]-[11]. In [12], an energy management system is proposed that is divided into several modules: forecasting, energy storage management, and an optimization module. The optimization module performs day-ahead unit commitment that uses information from load and distributed generation (DG), power forecasting module, market information, and energy storage management system to economically allocate generation in a microgrid. A power management strategy for wind-diesel-BESS systems is presented in [13]. Diesel and energy storage power setpoints are dispatched, using day-ahead wind and load forecasts, to minimize diesel generator operating costs, as well as, costs related to battery lifetime. A conceptual idea for multi-stage economic load dispatch in island microgrids is presented in [14]. To address the issues of variability and uncertainty, in [15]-[18], a model predictive control (MPC) approach is introduced. The strategy is based on dispatching power at minimal cost, assuming that energy storage is not available, that renewable sources are dispatchable, and that only short term wind forecasts are reliable.

In this work, a centralized MPC based coordination strategy is proposed for dispatch of DERs in an isolated system. One key difference between this work and that proposed in [15]-[18] is that performance objectives are incorporated in addition to economics. The goal of this work is to maximize the amount of wind generation in the system while considering system economics and the individual controls of the DERs. This can be done by formulating a look-ahead dispatch problem and casting it in a multi-objective framework. The objectives are to: minimize fuel costs of diesel generators, minimize changes in power output of diesel generators (reducing wear and tear), minimize costs associated with low battery life of energy storage, and to maximize the ability for generators to provide real-time balancing. Two control modes are adopted depending on whether the energy storage system used to compensate for wind or net load variability. Simulation studies are used to evaluate the performance of the different control strategies and to demonstrate the effectiveness of the closed loop MPC in compensating for uncertainties in wind and load forecasts.

This paper is organized as follows. In Section II, a brief description of the standard look-ahead dispatch problem is given. An optimal control coordination scheme using MPC is presented in Section III. In Section IV, case studies are presented that demonstrate the effectiveness of the optimal control coordination strategy. Finally, conclusions are given in Section V.

II. CLASSICAL DISPATCH PROBLEM FORMULATION

In a typical dispatch formulation with conventional generation, wind generation, and BESS, the objectives are to: 1) minimize fuel costs of diesel generators and 2) minimize operating costs of energy storage. The power outputs of the

diesel generators and energy storage are dispatched based on wind and load forecasts over an entire horizon. The optimization problem is formulated as follows:

$$\min_{P_{Gi}(k), P_s(k)} \sum_{k=1}^N \sum_{i=1}^G C(P_{Gi}(k)) + \sum_{k=1}^K C(P_s(k)) \quad (1)$$

subject to

$$\sum_{i=1}^G P_{Gi}(k) + \sum_{j=1}^{Gr} \hat{P}_{wj}(k) + P_s(k) = \hat{L}(k) \quad (2)$$

$$SOC(k) = SOC(k-1) - \alpha P_s(k-1) \quad (3)$$

$$P_{Gi}^{min} \leq P_{Gi}(k) \leq P_{Gi}^{max}, i = 1, 2, \dots, G \quad (4)$$

$$|P_{Gi}(k+1) - P_{Gi}(k)| \leq R_{Gi}^{max}, i = 1, 2, \dots, G \quad (5)$$

$$SOC_{min} \leq SOC(k) \leq SOC_{max} \quad (6)$$

The above constraints (2-6) are calculated for $k = 1, \dots, N$, where N is the length of the prediction horizon. The fuel cost of each generator $C(P_{Gi}(k))$ is assumed to be linear and is given by

$$C(P_{Gi}(k)) = a_i + b_i P_{Gi}(k) \quad (7)$$

where, a_i, b_i are the fuel cost coefficients. The cost associated with operating the BESS, $C(P_s(k))$, is given by the following expression which is adapted from [13]:

$$C(P_s(k)) = \pi_{SOC} SOC(k) C_p V_{max} \quad (8)$$

In (3), α is a constant given by $\alpha = \eta / (E_{max}) \Delta t$ where, Δt is the time step duration (hr). The objective function defined in (1) is convex, and hence, any standard quadratic programming solver can be used to obtain the optimal solution. The decision variables in the optimization problem are the power setpoints of energy storage and generators. The basic power balance equation is given by (2), which must be satisfied at every time step over the prediction horizon. The evolution of the state of charge at every time step is given by (3). Furthermore, at every time step, the current state of charge is a function of the state of charge of the previous time step, the storage charge/discharge power, and the energy capacity. The output power of the generators and state of charge of the storage are constrained with the limits defined in (4), (5) and (6).

III. OPTIMAL CONTROL OF DISTRIBUTED RESOURCES USING MODEL PREDICTIVE CONTROL

The look-ahead dispatch problem discussed earlier has inherent increased uncertainty with high penetration of renewable energy resources in the system and is implemented in an open-loop manner. The optimization problem is solved over an entire horizon once and the resulting sequence of control inputs are implemented at the corresponding time steps. Even though day-ahead forecasts for load demand are reliable, day-ahead forecasts for wind are not. One possible technique to solve this problem is to use MPC, where at every step a finite horizon optimal control problem is solved using feedback from the system. However, the control sequence is implemented for only one step ahead. In this manner, MPC is considered closed-loop and has the ability to compensate for additional uncertainty in demand variability caused by high penetration of renewable energy resources. The MPC based optimal control problem can be viewed as a multi-objective optimization problem with goals to: 1) minimize fuel costs of diesel generators, 2) minimize changes in power output of diesel generators reducing mechanical wear and tear, 3) minimize costs associated with low battery life of energy storage, and 4) minimize the inability of isochronous generators to provide real-time balancing. Isochronous control

of conventional generators is necessary because of mismatches between predictions and reality.

A. Description of Model Predictive Control

In the MPC approach, the control action at each step is computed on-line rather than using a pre-computed, off-line, control law. A model predictive controller uses, at each sampling instant, the system's current state, input and output measurements and the system's model to calculate, over a finite horizon, a future control sequence that optimizes a given performance index and satisfies constraints on the control action. The basic structure of a MPC controlled system, given that the system's states are available, is given in Fig. 1.

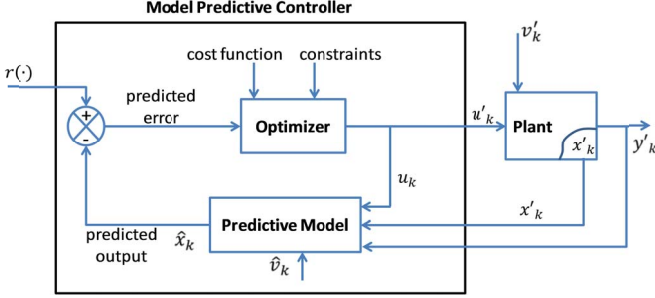


Fig.1 State feedback Model Predictive Controller

Consider the following discretized dynamic system $x'_{k+1} = f(x'_k, u'_k, v'_k)$, $y'_k = g(x'_k, u'_k)$ where x'_k are the state variables assumed to be measurable at every time step k , y'_k are the outputs of the system, and v_k is process noise, $f(\cdot)$ and $g(\cdot)$ are the functions relating state, control and noise variables to the states in the next step and outputs respectively. The control objective is to find a sequence of control inputs $u'(k)$, $u'(k+1), \dots, u'(k+N-1)$ over a given prediction horizon N such that a given cost function and constraints are satisfied. The above control sequence will result in a predicted sequence of state vectors which are given by $\hat{x}(k+1|k), \hat{x}(k+2|k), \dots, \hat{x}(k+N|k)$ which can then be used to compute the predicted sequence of system outputs $\hat{y}(k+1|k), \hat{y}(k+2|k), \dots, \hat{y}(k+N|k)$. Using this information, the control $u'(k)$ can be applied to the system to obtain x'_{k+1} . The process is repeated with measurement of x'_{k+1} serving as an initial condition to compute the control at the next step $u'(k+1)$. The model predictive controller can be described mathematically as follows:

$$\min_U J(\hat{X}, U) \quad (9)$$

$$\text{subject to: } \hat{x}_{k+1} = f(\hat{x}_k, u_k, \hat{v}_k) \quad (10)$$

$$\hat{y}_k = g(\hat{x}_k, u_k) \quad (11)$$

$$l(\hat{x}_k, \hat{x}_{k+1}, u_k, \hat{v}_k) = 0 \quad (11)$$

$$h(\hat{x}_k, \hat{x}_{k+1}, u_k, \hat{v}_k) \leq 0 \quad (12)$$

where $\hat{X} = [\hat{x}(k+1|k) \ \hat{x}(k+2|k) \ \dots \ \hat{x}(k+N|k)]^T$ and $U = [u'(k) \ u'(k+1) \ \dots \ u'(k+N-1)]^T$. The dynamics of the predictive model and constraints given in (10) – (12) are computed at every time step for $k = 0, 1, \dots, N-1$.

B. Look Ahead Dispatch using MPC

In this section, the look-ahead dispatch problem will be formulated as a model predictive control problem for the specific system considered. The three main components that need to be defined are the optimizer, predictive, and system models [20]. A different set of system and predictive models is

identified for when the storage is used to compensate for wind or net load variability.

System Model

The power system under consideration consists of two diesel generators, a battery energy storage system, a wind power plant, a mix of loads, and a dump load to represent real-time wind curtailment. Because the power dispatch is static in nature, static models are used to represent the system. Dynamics are introduced by set point changes of generators and storage threshold. Also, losses are neglected.

If the BESS is used to compensate wind variability, the storage unit will charge if wind generation is greater than a threshold and discharge if wind is less than the threshold value. On the contrary, if used to compensate net load variability (total load – wind power), the BESS will charge if net load is less than a threshold and vice versa. The diesel generators supply the remaining load that the wind and storage do not supply. Generator 2 is scheduled by the dispatch algorithm, while generator 1 is in charge of balancing the system because of uncertainties in wind and load. Dump load is incorporated since it is important to maintain generator 1 above a minimum loading requirement to allow for real-time balancing at all times.

The system dynamics for when energy storage is used to compensate for wind variability are given by

$$P_{G2}(k+1) = P_{G2}(k) + \Delta P_{G2}(k) \quad (14)$$

$$T(k+1) = T(k) + \Delta T(k) \quad (15)$$

$$SOC(k+1) = SOC(k) - \alpha(T(k) - P_w(k)) \quad (16)$$

$$P_{G1}(k) = -P_{G2}(k) - T(k) + P_L(k) \quad (17)$$

Notice that (17) represents the power balance of the system, and generator 1 is in charge of compensating any imbalance. The state variable, control input and disturbance vectors are defined as

$$x'_k = \begin{bmatrix} P_{G2}(k) \\ T(k) \\ SOC(k) \end{bmatrix}, u'_k = \begin{bmatrix} \Delta P_{G2}(k) \\ \Delta T(k) \end{bmatrix} \text{ and } v'_k = \begin{bmatrix} P_L(k) \\ P_w(k) \end{bmatrix}$$

and the output is taken to be $y'_k = P_{G1}(k)$. The dynamics (14)–(17) can be re-written in state space form

$$\begin{aligned} x'_{k+1} &= Ax'_k + Bu'_k + B_d v'_k \\ y'_k &= Cx'_k + D_d v'_k \end{aligned}$$

with

$$\begin{aligned} A &= \begin{bmatrix} 1 & 0 & 0 \\ 0 & 1 & 0 \\ 0 & -\alpha & 1 \end{bmatrix} & B &= \begin{bmatrix} 1 & 0 \\ 0 & 1 \\ 0 & 0 \end{bmatrix} & B_d &= \begin{bmatrix} 0 & 0 \\ 0 & 0 \\ 0 & \alpha \end{bmatrix} \\ C &= [-1 \ -1 \ 0] & D_d &= [1 \ 0] \end{aligned} \quad (18)$$

In the case when energy storage is used to compensate for net load variability, the dynamics of the state of charge given in (16) are modified to

$$SOC(k+1) = SOC(k) - \alpha(P_L(k) - P_w(k) - T(k)) \quad (19)$$

and $P_{G1}(k)$, given in (17) becomes

$$P_{G1}(k) = -P_{G2}(k) + T(k) \quad (20)$$

which gives the following system matrices

$$\begin{aligned} A &= \begin{bmatrix} 1 & 0 & 0 \\ 0 & 1 & 0 \\ 0 & \alpha & 1 \end{bmatrix} & B &= \begin{bmatrix} 1 & 0 \\ 0 & 1 \\ 0 & 0 \end{bmatrix} & B_d &= \begin{bmatrix} 0 & 0 \\ 0 & 0 \\ -\alpha & \alpha \end{bmatrix} \\ C &= [-1 \ -1 \ 0] & D_d &= [0 \ 0] \end{aligned} \quad (21)$$

Defining $P_{imbal} = -P_{G2}(k) - T(k) + P_L(k)$ based on equation (17) and $P_{imbal} = -P_{G2}(k) + T(k)$ based on equation (20); the dump load logic is defined as:

$$\begin{cases} \text{if } P_{imbal} < P_{G1min} \Rightarrow \begin{cases} P_{G1} = P_{G1min} \\ P_{dump} = P_{G1min} - P_{imbal} \end{cases} \\ \text{if } P_{imbal} \geq P_{G1min} \Rightarrow \begin{cases} P_{G1} = P_{imbal} \\ P_{dump} = 0 \end{cases} \end{cases} \text{ and}$$

When there is excessive wind generation ($P_{imbal} < P_{G1min}$), the dump load takes the balancing power. The dump load represents wind curtailment applied in real-time to maintain generator 1 balancing control. This dump load is useful to quantify the performance of the different coordination strategies being compared; the control strategy that minimizes the dump load is making better use of the wind resource.

Remark: Notice that there is a difference between the power balance of the actual system and the power balance constraint used in optimization (either classical or MPC). In optimization the power balance constraint is met for forecasted values of load and wind generation. In the actual system operation, there is a mismatch due to forecast errors that will be picked up by the generator/s in charge of system balance (e.g. by secondary frequency control). Therefore the actual power output of these generators will deviate from the optimal scheduled values. In the real time operation, if the generator/s in charge of frequency control reaches their minimum or maximum limits, frequency control can be lost and the system could exhibit frequency deviations (poor performance) as shown in [5] or frequency instability. In this paper we avoid generator 1 to reach the minimum output (avoiding loss of balancing control) by using a dump load to represent wind curtailment.

Predictive Model

In the predictive model, actual values at $k = 0$ are measured from the system and used as for initialization. States and disturbance predictions are made for times $k = 1, \dots, N - 1$. Hence, for the case when storage compensates for wind variability, the following dynamics of predictive values are defined:

$$\hat{P}_{G1}(k+1) = \hat{P}_{G1}(k) + \Delta P_{G1}(k) \quad (22)$$

$$\hat{P}_{G2}(k+1) = \hat{P}_{G2}(k) + \Delta P_{G2}(k) \quad (23)$$

$$\hat{T}(k+1) = \hat{T}(k) + \Delta T(k) \quad (24)$$

$$SOC(k+1) = SOC(k) - \alpha (\hat{T}(k) - \hat{P}_w(k)) \quad (25)$$

$$\hat{P}_{G1}(k) = -\hat{P}_{G2}(k) - \hat{T}(k) + \hat{P}_L(k) \quad (26)$$

where $(\hat{\cdot})$ are the predicted values of the quantities defined in (15) – (17). Hence, the predicted state variables, control input and disturbance vectors can be defined as

$$\hat{x}_k = \begin{bmatrix} \hat{P}_{G1}(k) \\ \hat{P}_{G2}(k) \\ \hat{T}(k) \\ SOC(k) \end{bmatrix}, u_k = \begin{bmatrix} \Delta P_{G1}(k) \\ \Delta P_{G2}(k) \\ \Delta T(k) \end{bmatrix} \text{ and } \hat{v}_k = \begin{bmatrix} \hat{P}_L(k) \\ \hat{P}_w(k) \end{bmatrix}$$

and the predicted output is taken to be $\hat{y}_k = \hat{P}_{G1}(k)$. The dynamics (22) - (26) can be re-written in state space form

$$\hat{x}_{k+1} = \hat{A}x_k + \hat{B}u_k + \hat{B}_d\hat{v}_k$$

$$y_k = \hat{C}x_k + \hat{D}_d\hat{v}_k$$

$$\hat{A} = \begin{bmatrix} 1 & 0 & 0 & 0 \\ 0 & 1 & 0 & 0 \\ 0 & 0 & 1 & 0 \\ 0 & 0 & -\alpha & 1 \end{bmatrix} \quad \hat{B} = \begin{bmatrix} 1 & 0 & 0 \\ 0 & 1 & 0 \\ 0 & 0 & 1 \\ 0 & 0 & 0 \end{bmatrix} \quad \hat{B}_d = \begin{bmatrix} 0 & 0 \\ 0 & 0 \\ 0 & 0 \\ 0 & \alpha \end{bmatrix}$$

$$\hat{C} = [0 \quad -1 \quad -1 \quad 0] \quad \hat{D}_d = [1 \quad 0] \quad (27)$$

When the energy storage unit is used to compensate for net load variability, the above matrices are modified to

$$\hat{A} = \begin{bmatrix} 1 & 0 & 0 & 0 \\ 0 & 1 & 0 & 0 \\ 0 & 0 & 1 & 0 \\ 0 & 0 & \alpha & 1 \end{bmatrix} \quad \hat{B} = \begin{bmatrix} 1 & 0 & 0 \\ 0 & 1 & 0 \\ 0 & 0 & 1 \\ 0 & 0 & 0 \end{bmatrix} \quad \hat{B}_d = \begin{bmatrix} 0 & 0 \\ 0 & 0 \\ 0 & 0 \\ -\alpha & \alpha \end{bmatrix}$$

$$\hat{C} = [0 \quad -1 \quad -1 \quad 0] \quad \hat{D}_d = [0 \quad 0] \quad (28)$$

The choice of the disturbance prediction models, v'_k , is also very important [20]. Autoregressive integrated moving average (ARIMA) and seasonal ARIMA (SARIMA) models were used for the prediction models of wind and load, respectively. These univariate time series models allow forecasted values to be calculated as a linear function of previous values. The Box-Jenkins [24] approach was used to select the parameters and orders of the models and to evaluate model adequacy.

Wind disturbance is modeled as an autoregressive integrated moving average (ARIMA) model

$$(1 - \sum_{i=1}^p \phi_i L^i)(1 - L)^d P_w(k) = (1 - \sum_{i=1}^q \theta_i L^i) \varepsilon(k) \quad (29)$$

where p, d , and q are the identified orders of the autoregressive (AR), integrated (I), and moving average (MA) parts, respectively. L is a lag operator, ϕ_i are the parameters of the AR part, θ_i are the parameters of the moving average part, and $\varepsilon(k)$ is the error term.

Since the load demand has a seasonal pattern, a seasonal ARIMA (SARIMA) model was used for the disturbance model

$$(1 - \sum_{i=1}^p \phi_i L^i)(1 - L)^d (1 - \sum_{i=1}^P \phi_{is} L^{is})(1 - L^s)^D P_L(k) = (1 - \sum_{i=1}^q \theta_i L^i)(1 - \sum_{i=1}^Q \theta_{is} L^{is}) \varepsilon(k) \quad (30)$$

where P, D, Q are the identified orders of the seasonal AR, I, and MA parts, respectively. L^s is the seasonal lag operator, s is the seasonal period, ϕ_{is} are the parameters of the seasonal AR part, θ_{is} are the parameters of the seasonal moving average part.

Optimizer

The look-ahead dispatch problem for optimal coordination of DERs can be re-formulated as a multi-objective optimization problem with the following cost function

$$J = \sum_{k=1}^N \left[w_1 (\hat{P}_{G1}(k) - P_{G1ref})^2 + w_2 (b_2 \hat{P}_{G2}(k) + b_1 \hat{P}_{G1}(k)) + w_3 (SOC(k) - SOC_{ref})^2 + w_4 (\Delta P_{G1}^2(k) + \Delta P_{G2}^2(k)) \right] \quad (31)$$

where w_1 penalizes the movement of the generator, in charge of real-time balancing, from a reference value to discourage minimum and maximum output values; w_2 is the penalty associated with fuel costs of diesel generators; w_3 is the penalty associated with low battery life; and w_4 is the weight penalizing the movement associated with the diesel generators. The conflicting objectives are to minimize the cost associated with maintaining the real-time balancing control, the movement of energy storage SOC, and the diesel generator movements and fuel costs. Rewriting (31) in terms of the state variables and control inputs of the predictive model gives

$$J(\hat{x}_k, u_k) = \sum_{k=1}^N [(\hat{x}_k - r)^T Q (\hat{x}_k - r) + c^T \hat{x}_k + u_k^T R u_k] \quad (32)$$

where

$$r = \begin{bmatrix} P_{G1ref} \\ 0 \\ 0 \\ SOC_{ref} \end{bmatrix} \quad c = \begin{bmatrix} w_2 b_1 \\ w_2 b_2 \\ 0 \\ 0 \end{bmatrix} \quad Q = \begin{bmatrix} w_1 & 0 & 0 & 0 \\ 0 & 0 & 0 & 0 \\ 0 & 0 & 0 & 0 \\ 0 & 0 & 0 & w_3 \end{bmatrix}$$

$$R = \begin{bmatrix} w_4 & 0 & 0 \\ 0 & w_4 & 0 \\ 0 & 0 & 0 \end{bmatrix}$$

Furthermore, the following constraints are imposed on the state variables

$$\begin{bmatrix} P_{G1min} \\ P_{G2min} \\ -\infty \\ SOC_{min} \end{bmatrix} \leq \begin{bmatrix} \hat{P}_{G1}(k) \\ \hat{P}_{G2}(k) \\ \hat{T}(k) \\ \hat{SOC}(k) \end{bmatrix} \leq \begin{bmatrix} P_{G1max} \\ P_{G2max} \\ \infty \\ SOC_{max} \end{bmatrix} \quad (33)$$

To solve this multi-objective optimization problem, the weighted sum method was chosen. The weight sum method is a classical and widely used method that scalarizes the set of objectives into a single-objective optimization problem by multiplying individual objectives by user defined weights. For example

$$U = \sum_{i=1}^m w_i F_i(x) \quad (34)$$

where m is the number of objectives functions, F_i is objective function i , w_i is the weight of objective function i , and U is the scalarized single objective function (utility function). The weights are chosen based on relative importance of the objectives. It is practical to first normalize the objectives using a function transformation [20] (i.e., dividing each objective function by the absolute maximum of the objective function),

$$F_i^{trans} = \frac{F_i(x)}{|F_i^{max}|} \quad (35)$$

where

$$\sum_{i=1}^m w_i = 1, \quad w_i \in [0,1] \quad (36)$$

Generally, if the objective function is convex and all weights are positive, minimizing (34) has sufficient conditions for Pareto optimality, but not the necessary conditions [20]. Therefore, *a priori* selection of weights does not guarantee an acceptable solution. Also, since all objectives are not of the same units, it is difficult to determine the relative importance of each objective to specify the best set weights that will optimize operations. For example, can one quantify how important economics is relative to maintaining system performance (i.e., frequency, real-time balance) or minimizing wear and tear of resources? The weights in this work are chosen arbitrarily by assuming the relative importance is known. Other multi-objective optimization techniques may need to be explored that do not require *a priori* information about the preferences of the decision maker and that can guarantee Pareto optimality. However, this is beyond the scope of this paper.

IV. SIMULATION STUDIES

A. Description of Test Cases

The test system consists of one diesel generator rated at 4MW, a diesel generator rated at 2.5 MW, a 3.6MWh rated BESS, a wind power plant (data obtained from [23]), dump load and an aggregate load of 1500 houses. System losses are neglected. One generator is in charge of real-time system balance, compensating for wind and load uncertainty not covered by the dispatch algorithms. The other generator operates at the given set points defined by the dispatch algorithm. The BESS can operate in two different control modes to compensate for: 1) net load variability or 2) wind variability given a threshold set point.

Several cases were considered as a proof of concept for the proposed optimal control strategy. Table I summarizes the different scenarios. The open loop and MPC look-ahead dispatch strategies were both applied to the test system for both BESS control strategies in the presence of high wind power production. For the open loop case, the look ahead dispatch formulation discussed in Section II was solved once for a 24-hr prediction horizon and the complete control sequence is implemented at the appropriate time. In order to quantify the performance of the closed-loop MPC strategy, different MPC prediction horizons are studied. These studies were performed for 10 min control steps and a 24 hr horizon.

TABLE I
SCENARIOS

| BESS control mode | Dispatch coordination strategy | Prediction horizon (steps) |
|--|--------------------------------|----------------------------|
| Case 1 - BESS compensates for wind variability | MPC look ahead-dispatch | 6 (1hr) |
| | Open loop look-ahead dispatch | 144 (24hr) |
| Case 2 - BESS compensates net load variability | MPC look ahead-dispatch | 4 (40min) |
| | | 6 (1hr) |
| | | 9 (1.5hr) |
| | | 12 (2hr) |
| | Open loop look-ahead dispatch | 144 (24hr) |

An ARIMA($p=2,d=1,q=0$) model was used for the wind forecast and a SARIMA($p=0,d=1,q=2,P=0,D=2,Q=2,s=144$) model was used for the load. The actual load and wind profiles are shown in Fig. 2. The actual versus predicted wind and load for a 24hr prediction horizon, using the ARIMA and SARIMA models, is shown in Fig. 3. The actual vs. predicted wind and load for a 6hr prediction horizon at every control step, using the ARIMA and SARIMA models, is shown in Fig. 4.

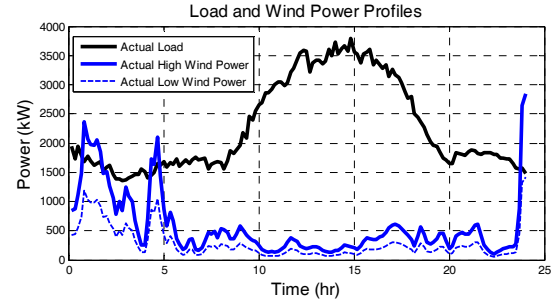


Fig. 2 Total Load and Wind Production

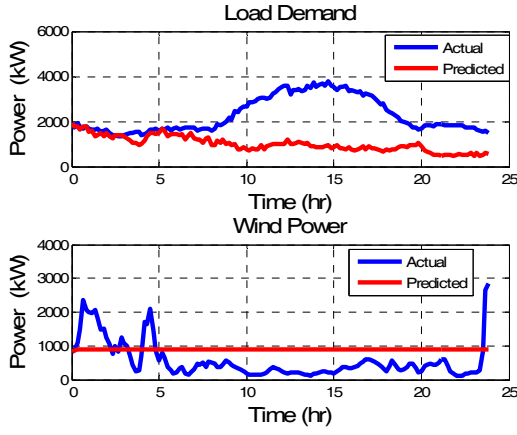


Fig. 3 Load and Wind Forecasts (24hr prediction horizon)

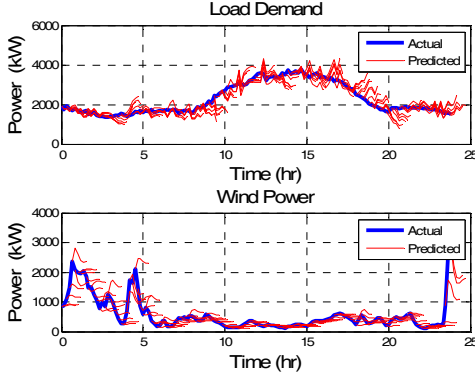


Fig. 4 Load and Wind Forecasts (1hr prediction horizon)

B. Compensating for Wind Variability

In this section, the performance of the closed-loop MPC look-ahead dispatch is compared to an open loop look-ahead dispatch for the case where the BESS is controlled to compensate for high wind variability.

The responses of the different DERs for the open loop case are shown in Fig. 5. The actual power output of generator 1 (performing real-time balancing) is very different from the predicted power output (Fig. 5a). Generator 1 balances power by compensating for large differences in the forecasted wind power and load demand. Generator 2 follows the set points given as expected (Fig. 5b). The actual SOC of the BESS is also very different from the predicted values (Fig. 5c). The BESS follows the actual wind variability until it discharges completely which is the point at which generator 1 supplies the additional power needed.

The responses of the different DERs for the closed-loop MPC case are shown in Fig. 6. The actual power output of generator 1 is, on average, closer to the predicted power output at each time step (Fig. 6a). This is because the difference between forecasted wind and load is much less in this case. Furthermore, unlike in the open loop case, generator 1 meets its control objective of balancing power and oscillates around the given reference value. Generator 2 follows the optimal set points given as expected (Fig. 6b). In contrast to the open loop case, the BESS actual SOC matches closely to the predicted values (Fig. 6c). This is because the forecasted wind and load deviate less from their actual values.

Furthermore, the BESS neither fully charges nor fully discharges.

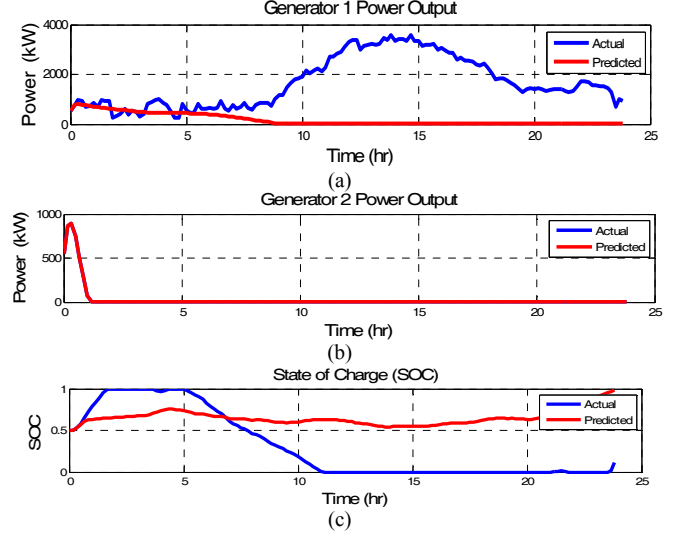


Fig. 5 Response to open loop dispatch when BESS compensates wind variability under high wind (a) Isochronous generator power output (b) power output of diesel generator 2 (c) BESS state of charge

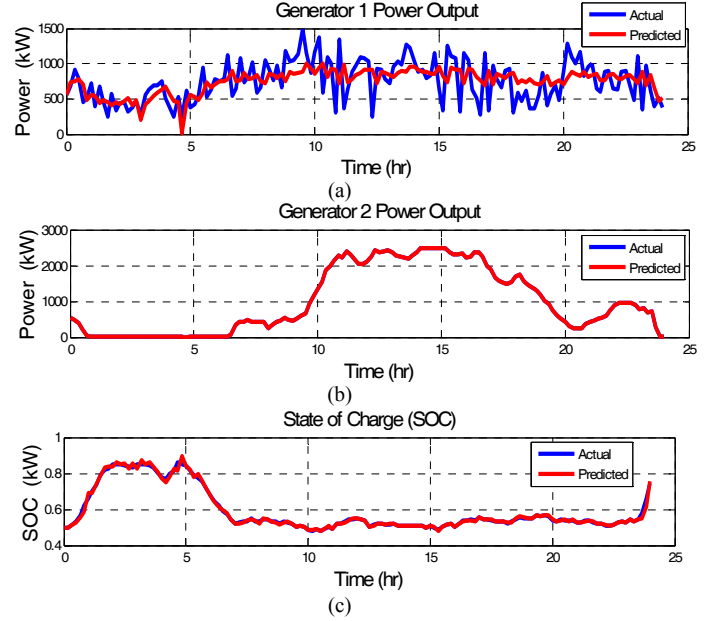


Fig. 6 Response to MPC when BESS compensates wind variability under high wind (a) Isochronous generator power output (b) power output of diesel generator 2 (c) BESS state of charge

The performance index (normalized total cost) is based on the specific weights chosen to for each objective defined in (31). For these studies, the following set of weights is chosen: $w_1=0.2$, $w_2=0.35$, $w_3=0.15$ and $w_4=0.3$. Calculating cost as defined by equation (31), the open loop cases shown have much higher costs (~three times greater), than the closed loop costs, as shown in Fig. 7a. The amount of dump load for the open and closed loop strategies is compared in Fig. 7b. The energy of the dumped load is much less in the closed loop case as compared to the open loop case, indicating that wind power resource is better utilized in the closed loop MPC coordination strategies.

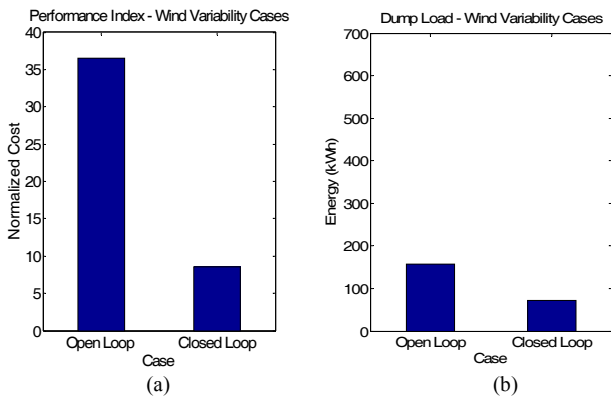


Fig. 7 Normalized total costs and dump load energy when BESS compensates wind variability under high wind

C. Compensating for Net load Variability

In this section, the open and closed loop responses of the different DERs are shown for the case where the BESS is controlled to compensate for net load variability. The responses of the different DERs for the open loop case are shown in Fig. 8. The isochronous generator initially follows its predicted power output exactly as seen in Fig. 8a. The overall response is similar to the wind variability open loop case. As shown in Fig. 8b, generator 2 also has a similar trend as compared to the wind variability case. The BESS has to account for the uncertainty in both wind and load forecasts and discharges faster compared to the wind variability open loop cases.

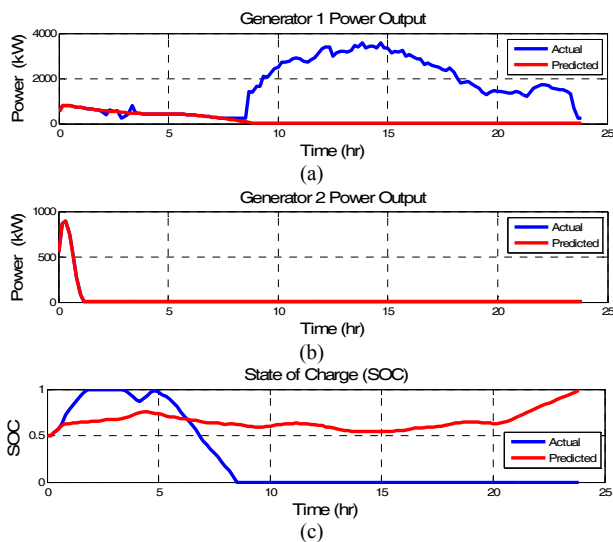


Fig. 8 Response to open loop dispatch when BESS compensates net load variability under high wind (a) Isochronous generator power output (b) power output of diesel generator 2 (c) BESS state of charge

The responses of the different DERs for the closed loop MPC case are shown in Fig. 9. Generator 1 follows its reference closely (Fig. 9a), unlike in the wind variability case (discussed in previous subsection). This is because the energy storage compensates for, wind and load variability, covering for most uncertainty. Similar to the wind variability closed loop case, the BESS follows its predicted output closely, as seen from Fig. 9c.

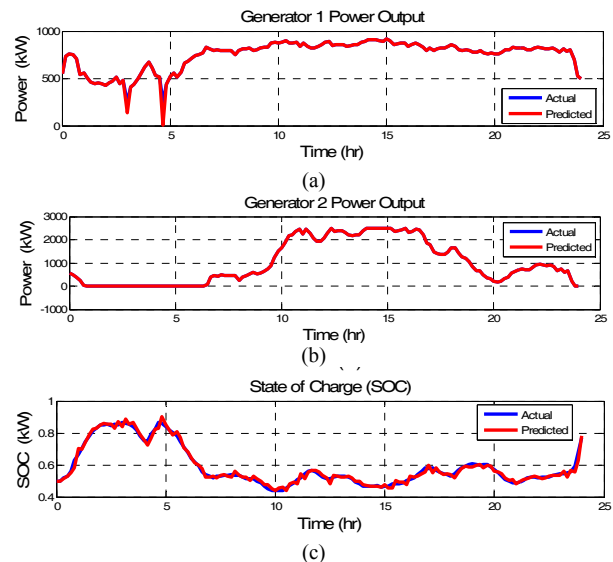


Fig. 9 Response to MPC when BESS compensates net load variability under high wind (a) Isochronous generator power output (b) power output of diesel generator 2 (c) BESS state of charge

The performance index and dump load energy are given in Figs. 10a and b. As in the wind variability case, the open loop cases shown have much higher costs than the closed loop MPC costs, as shown in Fig. 10a (calculating cost as defined by equation (31)). Also, the amount of dump load is much less in the closed loop MPC case as compared to the open loop case as seen from Fig. 10b. In the closed-loop case, the control strategy to compensate for net load variability performs better than the strategy to compensate for wind variability. The amount of energy dumped is also larger for the wind variability case indicating that the net load variability coordination strategy is more effective.

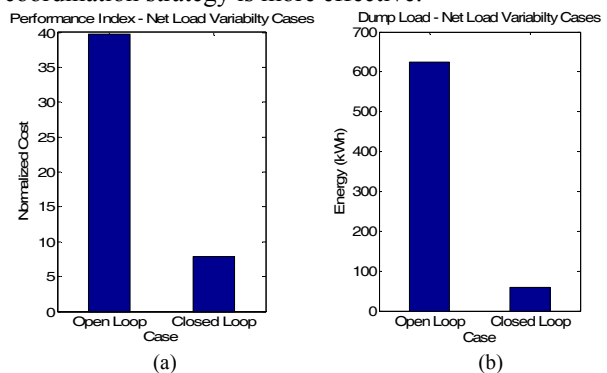


Fig. 10 Normalized total costs and dump load energy when BESS compensates net load variability under high wind

Next, the performance of the closed loop MPC strategy for different prediction horizons is shown in Fig. 11a. As the prediction horizon is increased, the performance improves because more information about the future is used, then the performance plateaus after a 1.5 hr (9 time steps) prediction horizon. However, dump load increases as the prediction horizon increases, because uncertainty increases (Fig. 11b). This implies that a longer prediction horizon does not improve the performance, nor does it maximize wind power use. A compromise between performance index and wind resource utilization (low dump load) is reached for 1.5 hr (9 time steps) prediction horizon.

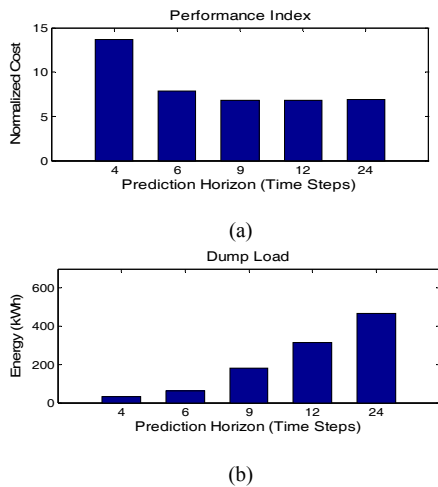


Fig. 11 Normalized total costs and dump load energy for different prediction horizons when BESS compensates net load variability under high wind

V. CONCLUSIONS

An optimal MPC-based control strategy is proposed for coordinating different DERs for an isolated power system. The designed MPC control strategy is able to meet all the performance objectives which are to minimize fuel costs and changes in power output of diesel generators (minimizing mechanical wear and tear), minimize costs associated with low battery life of energy storage, and to encourage normal system operation while maximizing the wind penetration in the system. The simulation studies indicate that the closed loop MPC strategy has a much better performance index than the open loop look-ahead dispatch under high wind penetration levels. It was also shown that the performance of the MPC was better for compensating net load variability as compared to compensating only wind variability. Simulations show that a compromise between performance index and wind resource utilization is reached for a particular value of look-ahead prediction horizon.

VI. ACKNOWLEDGEMENTS

The authors are grateful for the comments and feedback provided by Dr. Frank Tuffner at PNNL.

VII. REFERENCES

- [1] D. Hammerstrom, J. Brous, D. Chassin, G. Horst, R. Kajfasz, P. Michie, T. Oliver, T. Carlon, C. Eustis, O. Jarvegren, W. Marek, R. Munson, and R. Pratt, "Pacific Northwest GridWise Testbed Demonstration Projects; Part II. Grid Friendly Appliance Project," PNNL-17079, 2007, Pacific Northwest National Laboratory, Richland, WA.
- [2] M. Donnelly, D. Harvey, R. Munson, D. Trudnowski, "Frequency and stability control using decentralized intelligent loads: Benefits and pitfalls", *IEEE Power & Energy Society General Meeting*, July 2010.
- [3] K. Tanaka, M. Oshiro, S. Toma, A. Yona, T. Senjyu, T. Funabashi and C.-H. Kim, "Decentralized control of voltage in distribution systems by distributed generators", *IET Generation, Transmission & Distribution*, vol. 4, pp. 1251-1260, 2010.
- [4] Y. Zhu, and K. Tomovic, "Real-time control of Distributed Energy Resources", *IEEE Power & Energy Society General Meeting*, July 2010.
- [5] S. Lu, M. Elizondo, N. Samaan, K. Kalsi, E. Mayhorn, R. Diao, C. Jin and Y. Zhang, "Control Strategies for Distributed Energy Resources to Maximize the Use of Wind Power in Rural Microgrids," *IEEE Power & Energy Society General Meeting*, Detroit, July 2011.
- [6] N. Ardeshtna, H. Ma and B. Chowdhary, "The challenge of operating wind power plants within a microgrid framework", *Power and Energy Conference at Illinois*, Urbana-Champaign, IL, February 2010.

- [7] M. Shahabi, M. R. Haghifam, M. Mohamadian, and S. Nabavi-Niaki, "Microgrid Dynamic Performance Improvement Using a Doubly Fed Induction Generator," *IEEE Trans. on Energy Conv.*, vol. 24, no. 1, pp. 137-145, March 2009.
- [8] J. A. Peças Lopes, C. L. Moreira and A. G. Madureira, "Defining control strategies for microgrid islanded operation," *IEEE Trans. on Power Syst.*, vol. 21, no. 2, pp. 916-924, May 2006.
- [9] A. Mehrizi-Sani and R. Iravani, "Potential-function based control of a microgrid in islanded and grid-connected modes," *IEEE Trans. on Power Syst.*, vol. 25, no. 4, pp. 1883-1891, November 2010.
- [10] R. Majumder, B. Chaudhuri, A. Ghosh, R. Majumder, G. Ledwich and F. Zare, "Improvement of stability and load sharing in an autonomous microgrid using supplementary droop control loop," *IEEE Trans. on Power Syst.*, vol. 25, no. 2, pp. 796-808, May 2010.
- [11] M. Donnelly, D. Harvey, R. Munson, D. Trudnowski, "Frequency and stability control using decentralized intelligent loads: Benefits and pitfalls", *IEEE Power & Energy Society General Meeting*, 2010.
- [12] C. Chen, S. Duan, T. Cai, B. Liu and G. Hu, "Smart energy management system for optimal microgrid operation", *IET Renewable Power Generation*, vol. 5, pp. 258-267, 2011.
- [13] C. Abbey and G. Joos, "Sizing and power management strategies for battery storage integration into wind-diesel systems", *IEEE Conference on Industrial Electronics (IECON)*, 2008.
- [14] D. Olivares, C. Canizares and M. Kazerani, "A Centralized Optimal Energy Management System for Microgrids", *IEEE Power & Energy Society General Meeting*, 2011.
- [15] L. Xie, and M. Ilic, "Model predictive dispatch in electric energy systems with intermittent resources", *IEEE International Conference on Systems, Man and Cybernetics*, 2008.
- [16] L. Xie, J. Joo, and M. Ilic, "Integration of intermittent resources with price-responsive loads", *North American Power Symposium*, 2009.
- [17] L. Xie, and M. Ilic, "Model predictive economic/environmental dispatch of power systems with intermittent resources", *IEEE Power & Energy Society General Meeting*, 2009.
- [18] L. Xie, P. Carvalho, L. Ferreira, J. Liu, B. Krogh, N. Popli and M. Ilic, "Wind Integration in Power Systems: Operational Challenges and Possible Solutions", *Proc. of the IEEE*, vol. 99, Jan 2011
- [19] "GridLAB-D Residential Module User's Guild". Available: http://sourceforge.net/apps/mediawiki/gridlab-d/index.php?title=Residential_module_user%27s_guide
- [20] E. Camacho and C. Bordons, "Model predictive control", Springer, 1999.
- [21] F. Katiraei, and C. Abbey, "Diesel Plant Sizing and Performance Analysis of a Remote Wind-Diesel Microgrid," *IEEE Power & Energy Society General Meeting*, 2007.
- [22] R. Marler, and J. Arora, "Survey of multi-objective optimization methods for engineering", *Structural and Multidisciplinary Optimization*, vol. 26, pp. 369-395, 2003.
- [23] NREL wind data [Online], Available: http://wind.nrel.gov/Web_nrel
- [24] Lecture notes [Online], Available: www.tcd.ie/Economics/staff/frainj/main/...notes/UNIVAR4.pdf

VIII. BIOGRAPHIES

Ebony Mayhorn (S'08) is an Electrical Engineering Ph.D. candidate focusing in the area of Power Systems at Texas A&M University. Also, she is a Ph.D. intern at the Pacific Northwest National Lab.

Karanjit Kalsi (S'07, M'10) is a power systems research engineer at the Pacific Northwest National Lab, Richland, WA, USA.

Marcelo A. Elizondo (S'98, M'08) is a power systems research engineer at the Pacific Northwest National Lab, Richland, WA, USA.

Wei Zhang (S'06, M'10) is an Assistant Professor in the Department of Electrical and Computer Engineering, The Ohio State University

Shuai Lu (M'06) is a senior research engineer at the Pacific Northwest National Lab, Richland, WA, USA.

Nader Samaan (S'00, M'04) is a senior research engineer at the Pacific Northwest National Lab, Richland, WA, USA.

Karen L. Butler-Purry (SM'01) joined Texas A&M University in 1994, where she currently serves as Associate Provost for Graduate Studies and Professor in the Department of Electrical and Computer Engineering.